Coastal Engineering 42 (2001) 105–114

Coastal Engineering
An International Journal for Coastal, Harbour and Offshore Engineers

www.elsevier.com/locate/coastaleng

Infiltration effects on sediment mobility under waves

Peter Nielsen *, Sebastian Robert, Bettina Møller-Christiansen, Peggy Oliva

Department of Civil Engineering, The University of Queensland, St. Lucia Qld 4072, Brisbane, Australia

Received 12 August 1999; received in revised form 16 June 2000; accepted 18 June 2000

Abstract

Sediment mobility measurements with a horizontal sand bed under non-breaking waves are reported. Conditions include no seepage and steady downward seepage corresponding to head gradients up to 2.5. The results indicate that infiltration tends to inhibit sediment mobility for a horizontal bed of 0.2-mm quartz sand exposed to moderated wave induced bed shear stresses. The effect is weak for the parameter range of the present study. The two opposing effects of shear stress increase due to boundary layer thinning and the stabilizing downward drag are successfully accounted for through the modified Shields parameter of Nielsen [Nielsen, P., 1997. Coastal groundwater dynamics. Proc. Coastal Dynamics '97, Plymouth, ASCE, pp. 546–555] using coefficients derived from independent studies. That is, from the shear stress experiments of Conley [Conley, D.C., 1993. Ventilated oscillatory boundary layers. PhD Thesis, University of California, San Diego, 74 pp.] and the slope stability experiments of Martin and Aral [Martin, C.S. and M.M. Aral, 1971. Seepage force on interfacial bed particles. J. Hydraulics Div., Proc. ASCE, Vol. 97, No. Hy7, pp. 1081–1100].

1. Introduction

A complete description of beach morphodynamics must include a model of the sediment transport through and/or along the swash zone. Such a model is however still lacking for at least a couple of reasons. Firstly, the water motion in the swash zone is quite different from that in the inner surf zone and not well understood. In particular, the bed shear stresses have not been measured. Secondly, there is a possibility that flow perpendicular to the sand surface (in/ex filtration or ventilation) and/or strong horizontal pressure gradients near bore fronts could influence the sediment motion significantly in the swash zone.

There is no doubt that strong, artificially induced infiltration or exfiltration can have an effect on the stability and erosion/accretion rates of beaches. However, the available field evidence, e g, Dean (1989), Davis et al. (1992), Curtis et al. (1996) and Turner and Leatherman (1997), is still inconclusive with respect to the degree of beach-face stabilization afforded by artificial drainage systems. The field studies are complicated by the natural, variability of beach morphology. The evidence from laboratory experiments with beach profiles is also very complex. Thus, Oh and Dean (1992) observed that while

* Corresponding author. Tel.: +61-7-3365-3510; fax: +61-7-3365-4599.

E-mail address: p.nielsen@mailbox.uq.edu.au (P. Nielsen).

0378-3839/01/$ - see front matter
PII: S0378-3839(00)00051-X

an elevated back-beach watertable had the expected destabilizing effect at the toe of the beach, the upper portion of the beach-face was actually accreting faster. Turner and Masselink (1998) developed a simple swash zone sediment transport models which indicates that infiltration should have the effect of make the beach face steepen and/or accrete. This may well be the case for a sandy beach in near equilibrium conditions. However, it is also a common observation that beach faces tend to erode at the arrival of storms where the infiltration rate is high.

The present study considers a simpler scenario than swash zones. We study sediment mobility under regular, non-breaking waves over horizontal sand beds, and we attempt to develop a quantitative description based on new as well as previous data.

Although recent field measurements by Horn et al. (1998) indicate that strong destabilizing pressure gradients ($\mathrm{d}h^*/\mathrm{d}z < -1$) may occur during individual swash withdrawals on a rising tide, the present study is focussed on the possible effects of infiltration ($\mathrm{d}h^*/\mathrm{d}z > 0$). h^* is the piezometric head. Experiments with $\mathrm{d}h^*/\mathrm{d}z < 0$ are complicated by the phenomenon of piping, i e, the water moving upwards through preferred, more or less fluidized paths.

Baldock and Holmes (1998) performed small scale, flat bed laboratory experiments including some with $\mathrm{d}h^*/\mathrm{d}z < 0$. They found that the rate of in/ex-filtration changed the mode of sediment transport. That is, bulk motion of a top layer, many grain diameters thick, was sometimes observed during exfiltration or no seepage but was suppressed by infiltration. They also found that infiltration could suppress ripple formation completely. The bulk motion was never observed in the present study and ripple growth was not measurably affected. Nor were the equilibrium ripple dimensions, measured in extended experiments, measurably affected by the applied infiltration rates.

2. Two opposing effects of infiltration

The previous laboratory experiments which have been reviewed by Sleath (1984) and more recently by Baldock and Holmes (1998) do not give a clear cut quantitative answer as to the effect of infiltration on sediment transport rates. It is a complicated matter because there are two opposing effects at play: firstly, infiltration will make the boundary layer thinner and hence increase the shear stress. Secondly, infiltration will exert a stabilizing downward drag on the sediment. The relative importance of these two opposing effects depends on the density of the bed particles and on the permeability of the bed. This balance was investigated through steady pipe flow experiments by Martin (1970). He used quartz sand and nickel pellets of the same size (0.58 mm). These two materials have vastly different specific gravity, s: 2.65 and 8.75, respectively. Martin's experiments covered the range $0 < \mathrm{d}h^*/\mathrm{d}z < 20$. He found that for the heavy nickel particles, the overall effect of the infiltration was destabilization: More nickel moved in the horizontal pipe for a given pipe discharge when water was sucked down through the bed. He found the opposite overall effect with quartz: Less quartz was moved by a given pipe discharge when more water was sucked down through the bed.

To get to the essence of the problem and transfer experimental knowledge between different flow scenarios, e g, from Martin's pipe flow to a sea bed under waves or a swash zone it is necessary to formulate it in terms of fundamental parameters like the shear velocity u_{*0}. Unfortunately however, Martin did not give information from which u_{*0} can be reliably determined.

Nielsen (1997) suggested the use of the modified Shields parameter of the form:

$$\theta = \frac{u_{*0}^2\left(1 - \alpha\dfrac{w}{u_{*0}}\right)}{gd_{50}\left(s - 1 - \beta\dfrac{w}{K}\right)}, \tag{1}$$

to account for the combined effects of increased shear stress and downward drag due to infiltration. K is the hydraulic conductivity of the bed material and by Darcy's law we have $w/K = -dh^*/dz$, α and β are dimensionless coefficients giving the strength of the shear stress increase and the downward drag, respectively. Comparing with the usual (no ventilation) Shields parameter,

$$\theta = \frac{u_{*0}^2}{gd_{50}(s-1)}, \tag{2}$$

Eq. (1) shows the essence, in linearized form, of the two opposing effects of the vertical seepage velocity w (positive upwards). The extra term in the numerator quantifies the shear stress increase due to the thinning of the boundary layer while the last term in the denominator represents the effects of w on the effective weight of the grains.

3. Infiltration effects on the bed shear stress

Conley (1993) performed experiments on the relationships between peak shear stress and the dimensionless in/ex-filtration velocity $w/A\omega$ in oscillatory flows. A is the water particle semi excursion just above the boundary layer and ω is the angular velocity $2\pi/T$. The shear stress measurements were made with a hot film probe, flush mounted in a porous but non-mobile bed in an oscillatory flow. Conley's data for symmetrical flow, replotted in terms of w/u_{*0} rather than $w/(A\omega)$, are shown in Fig. 1. Subscript "0" corresponds to no ventilation, i e, $w = 0$.

The straight line, which approximates the data trend for small to moderate ventilation velocities, corresponds to:

$$\frac{\hat{\tau}}{\hat{\tau}_0} = 1 - 16\frac{w}{u_{*0}} \qquad \text{for } -0.05 < \frac{w}{u_{*0}} < 0.025; \tag{3}$$

or, with reference to Eq. (1):

$$\alpha = 16. \tag{4}$$

Although this α-value also works with the present sediment transport data, it would still be desirable to

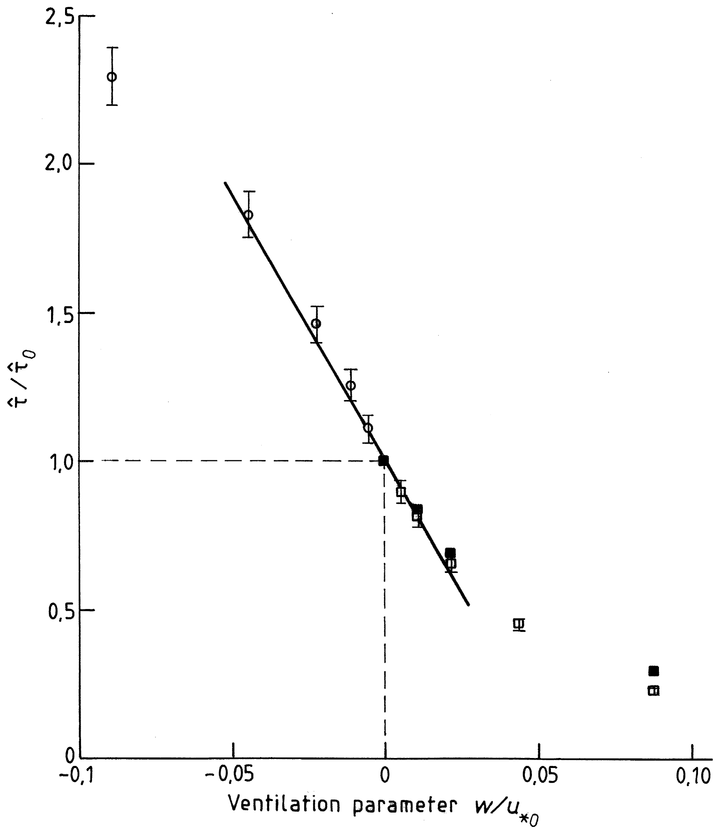

Fig. 1. Data of Conley (1993) from symmetrical wave motion over a flat, immobile, porous bed. The line corresponds to Eq. (3).

have data from real sand beds since they may behave very differently from fixed beds. Also, Conley's bed roughness would have been unrealistically small compared with movable sand beds. His measurements correspond to a friction factor f_w of only 0.004 while the smallest friction factor that has ever been measured over movable sand beds, including flat (non-rippled) beds, was about 0.03, eight times larger. See Nielsen (1992) p. 147.

4. Infiltration effects on the stability of surface particles

In the denominator of Eq. (1), the extra term quantifies the stabilizing effect of downward drag. The factor β which quantifies the increase of the particles weight due to the vertical seepage velocity is unity for particles within the bed, cf Nielsen (1992) p. 102, but considerably smaller for particles on the surface. Martin and Aral (1971) performed slope failure experiments which indicate that the appropriate β-value for particles on the surface is in the range:

$$0.35 < \beta < 0.4. \tag{5}$$

5. The magnitude of natural infiltration velocities

The most abundant data relating to the infiltration of water in the swash zone are watertable data. However, care must be taken when changes in watertable heights are interpreted into infiltration velocities. This was done by Kang et al. (1994). They rewrote the shallow aquifer watertable equation into the form:

$$\frac{\partial\eta}{\partial t} = \frac{KD}{n_e}\frac{\partial^2\eta}{\partial x^2} - \frac{w(x,t)}{n_e}, \tag{6}$$

where $\eta(x, t)$ is the watertable height, D is the undisturbed aquifer depth and n_e is the effective porosity. For laboratory experiments with regular waves where $\eta = \eta(x)$ was in equilibrium with the wave runup distribution, they obtained time-averaged infiltration velocities ranging up to 0.1 K. For the dynamic scenario during a rising tide in the field where the watertable rises rather rapidly, they found values in the range $0 < -w < 0.6$ K. The latter, unsteady values were however most likely too large because they were based on an effective porosity n_e equal to the total drainable porosity: $n_e = n = 0.3$. Sand column experiments by Nielsen and Perrochet (in press), on oscillating watertables and the associated effective porosity indicate the magnitude,

$$|n_e| = \frac{n}{\left(1 + 1.5\dfrac{\omega H_c}{K}\right)^{2/3}}, \tag{7}$$

for watertables well below the sand surface. For relatively fast oscillations (large $\omega H_c/K$), this may be very considerably smaller than the static effective porosity n. H_c is the capillary height of the beach sand. For watertables less than $0.5H_c$ below the sand surface the effective porosity was found to be even smaller, possibly as low as $(d_{50}/H_c)n$ when the watertable is only a few grain diameters below the sand surface.

What this means with respect to translating watertable change into infiltration rates is illustrated roughly if we ignore the middle term in Eq. (6), i e:

$$w \approx -n_e\frac{\partial\eta}{\partial t}. \tag{8}$$

That is, for a given measured rate of watertable rise the corresponding infiltration velocity is roughly proportional to the effective porosity.

Instead of deriving the infiltration velocity from watertable measurements one might instead use pressure-gradient measurements as done by Turner and Nielsen (1997) and Horn et al. (1998). This method is based on Darcy's law in the form:

$$w = -K\frac{\mathrm{d}h*}{\mathrm{d}z} = -K\frac{\mathrm{d}}{\mathrm{d}z}\left(\frac{p}{\rho g} + z\right), \tag{9}$$

i e, if pressures p_1 and p_2 have been measured a levels z_1 and z_2 in the same vertical the vertical flow rate in between must have been,

$$w = -K\frac{\dfrac{p2}{\rho g} + z_2 - \left(\dfrac{p1}{\rho g} + z_1\right)}{z_2 - z_1}. \tag{10}$$

Applying this method, Turner and Nielsen found peak infiltration velocities of the order .0003 m/s ≈

0.15 K coinciding with $(d\eta)/dt$-values of the order 0.07 m/s during a falling tide. Hence, the relevant effective porosity n_e would by the rule-of-thumb Eq. (8) have been about 0.004. Horn et al (1998) found similarly modest infiltration rates ($w < 0.15\ K$) generated by swash uprushes during a rising tide. However, during the following backwashes they found very considerable negative head gradients: $dh^*/dz < -2$! which lasted for the order of 5 s. This occurred when the pressure 5 mm below the sand surface dropped very rapidly to values below atmospheric while the pressure at -15 mm dropped much more slowly. These potentially very destabilizing, negative pressure gradients which exceed what would be required for fluidization of the bed are not well understood. This swash-phenomenon is not believed to have occurred in the permanently submerged sand bed of the present study.

6. Experimental setup

The experiments of the present study were done in the wave flume shown in Fig. 2. The wave periods were in the range 1.45 s $< T <$ 2.4 s where near-bed velocities of a reasonable magnitude can be generated without significant wave reflection. The experiments were done with well sorted ($d_{90}/d_{10} = 1.83$) quartz sand with $d_{50} = 0.20$ mm. The edges at the ends of the sand box were rounded in order to minimize scour.

Steady seepage could be generated by letting out water from the gravel layer under the sand bed. The seepage velocity w was then calculated as the seepage discharge divided by the sand bed area. At the same time, the piezometric head difference through the sand bed was measured by comparing the piezometric head in the gravel layer with the mean water level above.

7. Experimental procedure

The sand bed was flattened before each test and all sand was removed from the plywood bottom on either side of the sand bed. Waves were then generated for a time span long enough for measurable amounts (about 0.3 kg) of sand to move out of the sand box in either direction but not long enough for significant scour holes to develop. Ripples started to form but did not reach equilibrium height during the experiments.

The sand on the landward and seaward sides of the sand box were then extracted allowing the corresponding time-averaged transport rates Q_{LW} and Q_{SW} to be calculated.

If water was extracted through the sand bed, the flow rate per unit area (w) was measured together with the piezometric head difference through the sand.

The data is summarized in Table 1 below.

8. Data analysis

Near bed particle semi-excursions A and velocity amplitudes $A\omega$ were calculated from the tabulated (T, h, H) using linear wave theory. The fact that not all of the waves were of sinusoidal shape does not influence the following discussion of the influence of infiltration on the sediment mobility under otherwise identical conditions. For the purpose of calculating Shields parameters and friction velocities, the wave friction factor f_w was then calculated from:

$$f_w = \exp\left[5.5\left(\frac{2.5 d_{50}}{A}\right)^{0.2} - 6.3\right], \tag{11}$$

in accordance with Nielsen (1992) p. 25, i e, using a bed roughness of 2.5 grain diameters.It was decided to consider the sediment mobility in terms of the average $Q_{AV} = 0.5(Q_{LW} + Q_{SW})$ of the off-shore and on-shore net transport rates and its dimensionless equivalent:

$$\Phi_{AV} = \frac{Q_{AV}}{\sqrt{(s-1)gd^3}} = \frac{Q_{LW} + Q_{SW}}{2\sqrt{(s-1)gd^3}}. \tag{12}$$

This is a much more robust measure of sediment mobility than either of Q_{LW} and Q_{SW} because these are sensitive to subtle changes, with wave height, in crest/trough asymmetry and, to net circulation velocities which depend very strongly upon the amount of wave reflection.

Fig. 3 shows Φ_{AV} for the data from Table 1 plotted against the grain-roughness Shields parameter $\theta_{2.5}$. The open triangles are the experiments

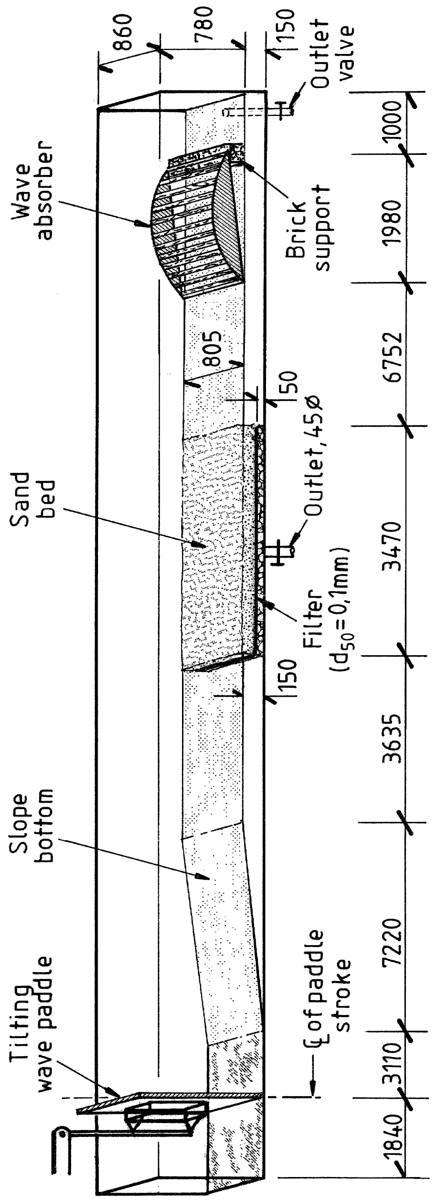

Fig. 2. Experimental setup for the present study.

Table 1
Summary of experimental results

T [s]	h [cm]	H [cm]	$10^6 \times Q_{SW}$ [m^2/s]	$10^6 \times Q_{LW}$ [m^2/s]	$10^6 \times Q_{AV}$ [m^2/s]	dh^*/dz [−]	w [mm/s]
1.78	45	10.38	0.14	0.07	0.11	0	0
1.78	45	12.73	0.23	0.60	0.42	0	0
1.78	45	14.96	0.79	1.12	0.96	0	0
1.45	50	19	0.73	2.04	1.39	0	0
1.45	50	20	0.60	1.63	1.12	0	0
1.45	50	14	0.11	0.29	0.20	0	0
1.45	50	11	0.01	0.04	0.03	0	0
1.45	50	11.3	0.02	0.14	0.08	0	0
1.45	50	17	0.68	0.99	0.84	0	0
1.45	50	19	0.64	2.02	1.33	0	0
1.45	50	15	0.15	0.78	0.46	0	0
1.45	50	13	0.08	0.43	0.26	0	0
1.4	50	22	1.03	2.29	1.66	0	0
1.8	45	19.3	1.47	1.51	1.49	0	0
1.8	45	23	2.65	2.39	2.52	0	0
1.8	45	24	2.61	2.65	2.63	0	0
1.8	45	17.33	1.12	1.00	1.06	0	0
1.8	45	20	1.92	1.97	1.95	0	0
1.8	45	22.7	2.20	2.45	2.33	0	0
1.8	45	22	1.66	2.18	1.92	0	0
2.4	45	7	0.00	0.09	0.05	0	0
2.4	45	11.2	0.08	0.46	0.27	0	0
2.4	45	13	0.52	1.07	0.80	0	0
2.4	45	17.3	0.74	2.31	1.52	0	0
1.86	45	4	0.00	0.02	0.01	0	0
1.86	45	4.8	0.03	0.55	0.29	0	0
1.78	45	10.38	0.06	0.07	0.06	1.82	−0.35
1.78	45	12.73	0.37	0.42	0.40	1.82	−0.35
1.78	45	14.96	0.55	0.96	0.76	1.82	−0.35
1.78	45	10.38	0.03	0.09	0.06	2.46	−0.48
1.78	45	12.73	0.26	0.37	0.31	2.46	−0.48
1.78	45	14.96	0.48	0.85	0.66	2.46	−0.48
1.45	50	15.5	0.13	0.47	0.30	0.5	−0.20
1.45	50	16.5	0.18	0.52	0.35	1.11	−0.22
1.45	50	13.3	0.03	0.07	0.05	1.11	−0.24
1.45	50	14	0.05	0.06	0.06	1.56	−0.26
1.43	50	17	0.47	0.85	0.66	1.44	−0.25
1.42	50	13.3	0.14	0.21	0.17	1.44	−0.25
1.8	45	19	1.26	1.28	1.27	1.22	−0.26
1.8	45	22.7	2.60	1.65	2.13	0.83	−0.26
1.8	45	23.3	2.31	2.30	2.31	1.22	−0.26
1.8	45	18	0.97	1.48	1.23	1.44	−0.23
1.8	45	20	1.83	2.18	2.01	1.55	−0.24
1.8	45	23	1.65	1.51	1.58	0.89	−0.24
1.8	45	23.3	1.78	2.40	2.09	1.3	−0.25
2.4	45	11.2	0.15	0.06	0.11	0.404	−0.08
2.4	45	13	0.26	0.25	0.25	0.404	−0.08
2.4	45	17.3	0.89	1.15	1.02	0.404	−0.08
2.4	45	11.2	0.03	0.02	0.03	0.54	−0.11
2.4	45	13	0.40	0.11	0.26	0.54	−0.11

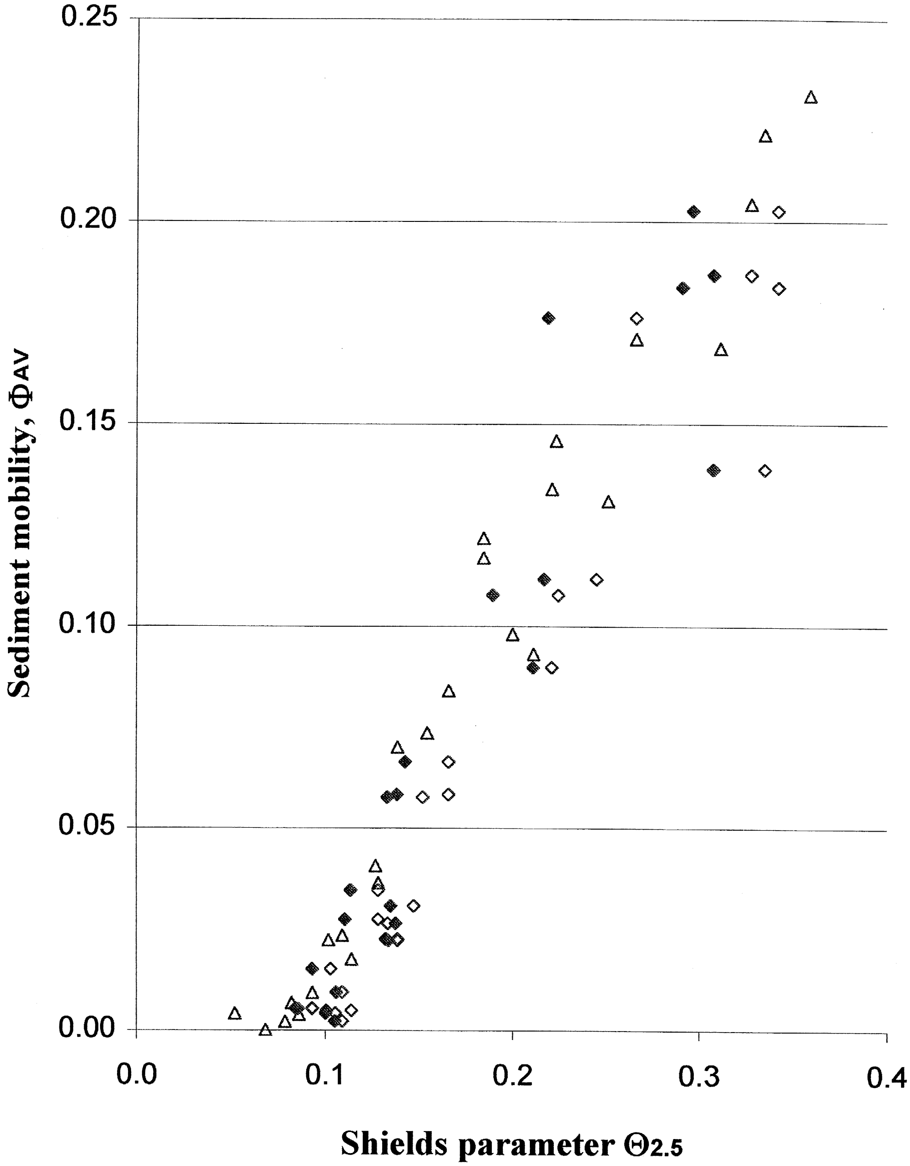

Fig. 3. Φ_{AV} vs. $\theta_{2.5}$ for the data in Table 1. Δ, no infiltration; $\Diamond$, infiltration $\theta_{2.5}$ uncorrected; $\blacklozenge$, infiltration $\theta_{2.5}$ corrected, in accordance with Eq. (1) and $(\alpha, \beta) = (16, 0.4)$.

without infiltration. The open diamonds are those with infiltration with Φ_{AV} plotted against the uncorrected Shields parameter. The filled diamonds show the experiments with infiltration but with the Shields parameter corrected in accordance with Eq. (1) and $(\alpha, \beta) = (16, 0.4)$.

Despite the scatter, we see that the uncorrected data with infiltration ($\Diamond$) lie to the lower right of the "no infiltration data" (Δ). Thus, the net effect of infiltration is to reduce the mobility of this 0.2-mm quartz sand. The full diamonds ($\blacklozenge$) which are the "infiltration data" plotted against the corrected Shields parameter (Eq. (1)) are seen to be on the same trend line as the "no infiltration data". Hence, Eq. (1) with $(\alpha, \beta) = (16, 0.4)$ accounts effectively for the effects of infiltration on sediment mobility.

9. Conclusions

The present data show that the corrections to the Shields parameter specified by Eq. (1) with $(\alpha, \beta)=(16, 0.4)$ bring the data from experiments with and without steady infiltration together around the same curve. The fact that these (α, β) values were determined by other authors in experiments of different kinds lends a bit of extra credibility to the underlying philosophy — they were not ad hoc values chosen to fit the present study.

While the experiments presented in Fig. 3 were all performed with 0.2-mm quartz sand and within a limited range of wave periods this conclusion is likely to have a fairly wide applicability because of the general nature of the formulae. They are also likely to be indicative of the effects of moderate exfiltration without piping or bulk motion.

While the overall effect of infiltration on 0.2-mm quartz sand is to impede the sediment motion, the net effect could well be an enhancement for pebbles or gravel (as it was for Martin's Nickel sediment). According to Eq. (1) the direction of the net effect depends on whether the ratio,

$$\frac{(s-1)\left(1-\alpha\frac{w}{u_{*0}}\right)}{\left(s-1-\beta\frac{u_{*0}}{K}\frac{w}{u_{*0}}\right)}, \tag{13}$$

(the ratio between the corrected and the uncorrected shields parameters) increases or decreases with increasing infiltration. Through differentiation of Eq. (13) and a little bit of manipulation, this leads to the following rule: Infiltration enhances sediment mobility for dense, coarse sediment with $\alpha(s\text{-}1) > \beta(u_{*0}/K)$ and impedes sediment motion for fine, light sediment with $\alpha(s\text{-}1) < \beta(u_{*0}/K)$.

We note that the experiments of the present study are an indication about sediment mobility only, not about the direction of the net sediment transport.

The difference in trends between the data with and without infiltration in Fig. 3 is small. Hence, if these experiments (with non-breaking waves over horizontal beds) are indicative for the processes in swash zones, we would expect the effects of infiltration on sediment mobility to be minor also in swash zones. That is, if the infiltration rates are in the range of $w/K < 0.2$ as observed by Kang et al. (1994) and by Turner and Nielsen (1997). However, strong destabilizing pressure gradients like those indicated by the swash zone measurements of Horn et al. (1998) might have very significant effects. The nature of these strong destabilizing pressure gradients and their causes are still largely unresolved and should be further investigated.

Also, the fluidizing effects of large horizontal pressure gradients near bore fronts need to be investigated. Clearly, if the beach face tends to be fluidized during the backwash by the "Horn et al pressure gradients" (Horn et al., 1998), a similar mechanism must exist, which enhances sediment transport during the uprush — otherwise all beach sand would quickly go offshore. The balancing effect might be delivered by fluidization due to strong horizontal pressure gradients during uprush. Sleath (1984) (p. 262), states that the requirement derived by Madsen (1974) for fluidization by horizontal pressure gradients is roughly,

$$\frac{\mathrm{d}h*}{\mathrm{d}x} \approx 0.6, \tag{14}$$

a value very likely to be exceeded near bore fronts in the swash zone.

Acknowledgements

This study was supported by the NICOP program of the US Office of Naval Research, Grant no. N00014-97-1-0793.

References

Baldock, T.E., Holmes, P., 1998. Seepage effects on sediment transport by waves and currents. Proc. 26th Int. Conf. Coastal Engineering, Copenhagen. ASCE, pp. 3601–3614.

Conley, D.C., 1993. Ventilated oscillatory boundary layers. PhD Thesis, University of California, San Diego, 74 pp.

Curtis, W.R., Davis, J.E., Turner, I.L., 1996. Independent evaluation of a beach dewatering system: Nantucket Island, Massachusetts. Proc 25th Int Conf Coastal Engineering, Orlando. ASCE, pp. 2677–2690.

Davis, G.A., Hanslow, D.J., Hibbert, K., Nielsen, P., 1992. Gravity drainage: A new method of beach stabilization through drainage of the watertable. Proc 23rd Int. Conf. Coastal Engineering, Venice. ASCE, pp. 1129–1141.

Dean, R.G., 1989. Independent analysis of beach changes in the vicinity of the Stabeach System at Sailfish Point, Florida. Consultants report 15 pp.

Kang, H.Y., Nielsen, P., Hanslow, D.J., 1994. Watertable overheight due to wave runup on a sandy beach. Proc. 24th Int. Conf. Coastal Engineering, Kobe. ASCE, pp. 2115–2124.

Horn, D.P., Baldock, T.E., Baird, A.J., Mason, T.E., 1998. Field measurements of swash induced pressures within a sandy beach. Proc. 26th Int. Conf. Coastal Engineering, Copenhagen. ASCE, pp. 2812–2825.

Madsen, O.S., 1974. Stability of a sand bed under breaking waves. Proc. 14th Int. Conf. Coastal Engineering, Copenhagen. ASCE, pp. 776–794.

Martin, C.S., 1970. Effect of a porous sand bed on incipient sediment motion. Water Resour. Res. 6 (4), 1162–1174.

Martin, C.S., Aral, M.M., 1971. Seepage force on interfacial bed particles. J. Hydraul. Div., Proc. ASCE 97 (Hy7), 1081–1100.

Nielsen, P., 1992. Coastal Bottom Boundary Layers and Sediment Transport. World Scientific, Singapore, 324 pp.

Nielsen, P., 1997. Coastal groundwater dynamics. Proc. Coastal Dynamics '97, Plymouth. ASCE, pp. 546–555.

Nielsen, P. and P. Perrochet. Capillary fringes and effective porosities for oscillating watertables. Water Resources Research (in press).

Oh, T.-M. and R.G. Dean, 1992. Beach face dynamics as affected by groundwater table elevations. Tech Report UFL/COEL-92/004, Dept. of Coastal and Oceanographical Engineering, University of Florida, 35 pp.

Sleath, J.F.A., 1984. Sea Bed Mechanics. Wiley, 335 pp.

Turner, I.L., Nielsen, P., 1997. Rapid watertable fluctuations: implications for swash zone sediment mobility. Coastal Eng. 32, 45–59.

Turner, I.L., Leatherman, S.P., 1997. Beach dewatering as a soft engineering solution to coastal erosion – a history and critical review. J. Coastal Res. 13 (4), 1050–1063.

Turner, I.L., Masselink, G., 1998. Swash infiltration–exfiltration and sediment transport. J. Geophys. Res. 103 (C13), 30,813–30,824.